Side-Chain Conformational Thermodynamics of Aspartic Acid Residue in the Peptides and Achatin-I in Aqueous Solution

Tomohiro Kimura, Nobuyuki Matubayasi, and Masaru Nakahara
Institute for Chemical Research, Kyoto University, Uji, Kyoto, Japan

ABSTRACT Sequence-position dependence of the side-chain conformational equilibrium of aspartic acid (Asp) residue is investigated for both model Asp peptides (di- to tetra-) and neuropeptide achatin-I (Gly-D-Phe-Ala-Asp) in aqueous solution. The *trans*-to-*gauche* conformational changes on the dihedral angle of C–C_α–C_β–C are analyzed in terms of the standard free energy ΔG^0, enthalpy ΔH^0, and entropy $-T\Delta S^0$. The thermodynamic quantities are obtained by measuring the dihedral-angle-dependent vicinal ^{1}H-^{1}H coupling constants in nuclear magnetic resonance over a wide temperature range. When the carboxyl groups of Asp are ionized, ΔG^0 in the aqueous phase depends by ~1–2 kJ mol^{-1} on the sequence position, whereas the energy change ΔE^0_{gas} in the gas phase (absence of solvent) depends by tens of kJ mol^{-1}. Therefore, the weak position dependence of ΔG^0 is a result of the compensation for the intramolecular effect ΔE^0_{gas} by the hydration ΔG^0_{hyd} ($= \Delta G^0 - \Delta E^0_{gas}$). The ΔH^0 and $-T\Delta S^0$ components, on the other hand, exhibit a notable trend at the C-terminus. The C-terminal ΔH^0 is larger than the N- and nonterminal ΔH^0 values due to the intramolecular repulsion between α-CO_2^- and β-CO_2^-. The C-terminal $-T\Delta S^0$ is negative and larger in magnitude than the others, and an attractive solute-solvent interaction at the C-terminus serves as a structure breaker of the water solvent.

INTRODUCTION

The role of hydration in determining the conformational equilibria of peptides and proteins in aqueous solution is a fundamental biophysical subject in structural biology. In a previous work (Kimura et al., 2002) we elucidated the competing role of hydration against the large intramolecular electrostatic energies in the side-chain conformational equilibria of such amino acids as aspartic acid (Asp) and asparagine (Asn), that involve the ionic carboxyl and polar amide groups in the side chain, respectively. In this work, we target a sequence-position dependence of the hydration effect for Asp side-chain conformational equilibria in both model and natural peptide systems. A series of Asp di-, tri-, tetra-, and achatin-I (Gly-D-Phe-Ala-Asp) peptides were investigated by measuring the dihedral-angle-dependent vicinal ^{1}H-^{1}H coupling constants in nuclear magnetic resonance (NMR) over a wide temperature range. The side-chain conformational study for the ionic peptides without explicit secondary structures is expected to provide insightful concepts on the structures of larger protein systems, since most of the ionic side chains are exposed to the solvent environment on the protein surface.

Although the large intramolecular electrostatic interaction energy in Asp and Asn monomers was considered as the dominant factor controlling the equilibria (Taddei and Pratt, 1964; Pachler, 1967; Dale and Jones, 1975; Kainosho and Ajisaka, 1975), it was revealed by combining NMR experiments with ab initio energy calculations that the hydration free energy competes against the intramolecular energy (Kimura et al., 2002). A degree of separation of positive and negative partial charges within the conformers was found to have a correlation with the hydration effect. In researches on simpler ionic systems of succinic acid (Nunes et al., 1981; Lit et al., 1993; Kent et al., 2002) and β-alanine (Gregoire et al., 1998; Nielsen et al., 2000), furthermore, there are accumulating observations implying that the hydration effect is as large as the intramolecular electrostatic interaction energy between vicinal ionic groups. As seen in Fig. 1 *a*, the charges in the Asp residues contained in peptides depend on the sequence positions; both positive and negative at the N-terminus, one negative at the nonterminus, and two negative at the C-terminus. There then arises a question concerning the sequence-position dependence of the electrostatic hydration effect on the ionic groups.

To discuss the hydration effect on the charged groups as separated from the intramolecular effect of electrostatic interactions, we need to calculate the conformational energy change (ΔE^0_{gas}) in the gas phase (see the conformers in Fig. 1 *b*). By combining the experimental free energy (ΔG^0) in aqueous solution and the calculated energy ΔE^0_{gas} in the gas phase, we can separately obtain the hydration free energy (ΔG^0_{hyd}) by $\Delta G^0 - \Delta E^0_{gas}$. Evaluation of ΔE^0_{gas} in comparison to ΔG^0 at every sequence position is thus the route to elucidating the position dependence of the hydration effect ΔG^0_{hyd}.

The sequence-position dependence of conformational equilibrium is further inspected by decomposing ΔG^0 into the enthalpic (ΔH^0) and entropic ($-T\Delta S^0$) components. Enthalpic contribution of the hydration effect (ΔH^0_{hyd} ($= \Delta H^0 - \Delta E^0_{gas}$)) can be examined through the observed ΔH^0 by referring to ΔE^0_{gas}, as in the case of the hydration free energy ΔG^0_{hyd} ($= \Delta G^0 - \Delta E^0_{gas}$). Major attention here is on whether or not the expected large position dependence of the intramolecular effect ΔE^0_{gas} is reflected in the total

Submitted June 24, 2003, and accepted for publication October 9, 2003.

Address reprint requests to Masaru Nakahara, Institute for Chemical Research, Kyoto University, Uji, Kyoto 611-0011, Japan. Tel./Fax: 81-774-38-3070; E-mail: nakahara@scl.kyoto-u.ac.jp.

0006-3495/04/02/1124/14 $2.00

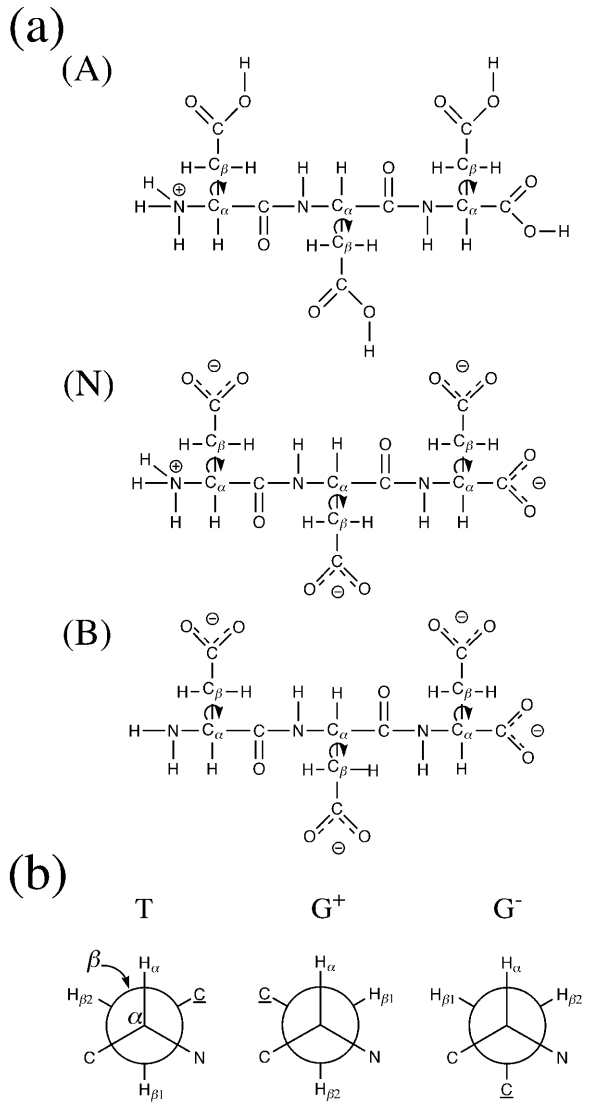

FIGURE 1 (*a*) Molecular structures of Asp tripeptide (A) at the acidic pD, (N) at the neutral pD, and (B) at the basic pD. The arrows represent the dihedral angles analyzed. (*b*) Staggered side-chain conformers of Asp with respect to the dihedral angles analyzed. C represents the β-carboxyl carbon in the side chain. N represents the α-amino nitrogen or α-amide nitrogen in the peptide bond, and C represents the α-carboxyl carbon or α-carbonyl carbon in the peptide bond.

conformational enthalpy ΔH^0. On the other hand, the entropic component $-T\Delta S^0$ in aqueous solution is dominated by the hydration effect. In this case, a correlation with the intramolecular charge distribution is of particular interest. There were reports of the side-chain ΔH^0 and $-T\Delta S^0$ for cyclic dipeptide systems involving aromatic amino acid residue(s) (Kopple and Marr, 1967; Kopple and Ohnishi, 1969); a magnetic anisotropy due to the aromatic ring(s) enabled to detect, through the ^{1}H chemical shifts, the temperature effect on the conformational ΔG^0. In this work, a high frequency resolution of the order of 0.01 Hz has made it possible to sensitively detect the temperature effect on the vicinal ^{1}H-^{1}H coupling constants; ΔH^0 and $-T\Delta S^0$ were separated in aqueous solution without special designing of the peptides examined.

Next question is whether the trends of position dependence of ΔG^0, ΔH^0, and $-T\Delta S^0$ found in the model Asp peptides are common to a natural peptide with biological functions. We choose achatin-I (Gly-D-Phe-Ala-Asp) to examine this point. It is known as a neuroexcitatory peptide of four amino acid residues, which was isolated from the ganglia of African snail, *Achatina fulica* Férussac (Kamatani et al., 1989). This peptide contains an ionic side chain in the C-terminal Asp. Since many of the neurotransmitters are characterized by the ionic groups involved, it is also of significance to investigate the role of Asp in achatin-I with regard to the structure-activity relationship of neuroexcitation. Indeed, the replacement of the C-terminal Asp by Asn leads to a decrease of the achatin-I activity, inducing a current on the neuron due to Na^+ ions (Kamatani et al., 1989; Kim et al., 1991). When achatin-I binds to the receptor with a suitable conformation, the water molecules strongly hydrated to the ionic groups need to be released; the binding phenomenon is a competing process against the hydration. Thus, the investigation of hydration effect on the conformational equilibrium of the peptide in bulk solution is indispensable to the understanding of the binding characteristics to the receptor.

METHODS

Materials

L-Aspartic acid (Asp) dipeptide (Asp-Asp), Asp tripeptide (Asp-Asp-Asp), Asp tetrapeptide (Asp-Asp-Asp-Asp), and achatin-I peptide (Gly-D-Phe-Ala-Asp) ammonium salt were from Sigma Chemical (St. Louis, MO). These materials were used without further purification. Deuterium oxide (D_2O, 99.90% D) solvent was from Euriso-top (Saint Aubin, France). D_2O solutions of DCl (18 wt %) and NaOD (40 wt %) used to control the solution pD (pH) were from Aldrich Chemical (Milwaukee, WI).

The aqueous solutions were prepared at 20 mM for the dipeptide, 10 mM for the tripeptide, 5 mM for the tetrapeptide, and 2 mM for the achatin-I peptide. At these concentrations, the effect of intermolecular interactions among the solutes on the side-chain conformational equilibria can be neglected.

The ionization states of the carboxyl and amino groups in the peptides were changed by adding the DCl or NaOD solution, and pD values were obtained by adding 0.4 units to the readings of the pH meter with a glass electrode (HORIBA, Model D-21, Kyoto, Japan; see also Glasoe and Long, 1960). The pD conditions examined were as follows: for the di-, tri-, tetra-, and achatin-I peptides, respectively, pD = 0.6, 0.6, 0.7, and 0.7 for the acidic conditions (A), pD = 6.5, 6.6, 7.3, and 7.5 for the neutral conditions (N), and pD = 13.0, 13.3, 13.6, and 13.8 for the basic conditions (B). The dominant ionization states of the carboxyl and amino groups in the peptides were identified by the geminal coupling constants to be (CO_2D, ND_3^+) at the acidic pDs, (CO_2^-, ND_3^+) at the neutral pDs, and (CO_2^-, ND_2) at the basic pDs; see Fig. 1 *a* for the representative case of the tripeptide in H_2O. Note that the ionization states of all the β-carboxyl groups at the N-, non-, and C-terminal positions are identical at each of the acidic, neutral, and basic conditions.

NMR measurements

^{1}H NMR of the aqueous solutions of the di-, tri-, and achatin-I peptides were measured on a 270-MHz FT-NMR spectrometer (JEOL USA, Model JNM-EX270, Peabody, MA). For the Asp tetrapeptide, the measurements were performed on a 600-MHz FT-NMR spectrometer (JEOL, Model JNM-LA600). The measurements were carried out at the acidic, neutral, and basic pD at 30°C to examine the ionization effect of the carboxyl and amino groups on the conformer distributions at room temperature. In the cases where the signal overlaps with that of solvent at 30°C, the measurements were carried out at 25°C by shifting the temperature-sensitive solvent signal downfield.

To separate the enthalpic and entropic contributions to the conformational equilibria, we examined the temperature effect on the conformer distributions at the acidic and neutral pD, focusing on the ionization effect of the carboxyl groups. As will be shown in the later section, the ionization effect of the N-terminal amino group is much smaller than that of the carboxyl groups even at the N-terminus. Thus, we limited the temperature study here to the acidic and neutral pD. The temperature range examined was 10–95°C at an interval of 5 or 10°C. The uncertainties were ±0.1°C. Free-induction decay signals were taken after >30 min of the temperature change except at the acidic pD above 70°C, where the signals were taken after ~5 min. The reduced waiting time was to avoid the peptide-bond decomposition; at >70°C, some signal overlap accompanying the peptide-bond decomposition was observed within 30 min after the temperature change, whereas the overlap was not detected at 60°C after more than a few hours. It was confirmed that the reduction of waiting time to ~5 min did not affect the accuracy of the coupling constants. At each temperature, the measurement was repeated two or three times. The temperature effect was investigated on the 270-MHz spectrometer for the di- and achatin-I peptides and on the 600-MHz spectrometer for the tri- and tetrapeptides.

The frequency resolution in the measurements was set to 0.01 Hz for the 270-MHz spectrometer and to 0.02 Hz for the 600-MHz spectrometer to evaluate the ^{1}H-^{1}H coupling constants. The high digital resolutions were achieved by sampling data of 131,072 points. The spectrum width was 1200–1960 and 2000–3200 Hz for the 270- and 600-MHz spectrometers, respectively, depending on the sample. All of the observable ^{1}H signals for the peptides appear within the spectrum ranges set. The spectrum for the analysis of coupling constants was obtained without an external chemical-shift reference to avoid the deterioration of the magnetic field uniformity and the overlap with the peptide signals. When the chemical shift values were to be recorded, the spectrum was obtained with a reference; 100 mM sodium 2,2-dimethyl-2-silapentane-5-sulfonate (DSS) D_2O solution contained in a 1.5-mm ID glass tube was set concentrically in a 10-mm OD NMR sample tube. The digital resolution here was set to 0.33 and 0.37 Hz for the 270- and 600-MHz spectrometers, respectively.

Conformational analysis

^{1}H NMR signals from each Asp residue of the peptides in aqueous solution show an ABX-type 12- or 5-line fine structure due to the coupling of one α- and two β-protons. The analysis of the ABX-type fine structure provides the vicinal ($J_{\alpha\beta1}$ and $J_{\alpha\beta2}$) and geminal ($J_{\beta1\beta2}$) coupling constants among the three protons (Pople et al., 1959). From the vicinal $J_{\alpha\beta1}$ and $J_{\alpha\beta2}$, the side-chain conformer probabilities on the C_α–C_β bond were determined by applying the three-staggered-state model for the conformers shown in Fig. 1 *b* (Pachler, 1964). The conformational analysis has its basis on the Karplus equation, which describes a dihedral-angle dependence of the vicinal coupling constants (Karplus, 1959, 1963). According to the three-staggered-state model, the observed $J_{\alpha\beta1}$ and $J_{\alpha\beta2}$ are expressed as

$$J_{\alpha\beta1} = P(\mathrm{T})J_\mathrm{t} + P(\mathrm{G}^+)J_\mathrm{g} + P(\mathrm{G}^-)J_\mathrm{g} \quad (1a)$$

$$J_{\alpha\beta2} = P(\mathrm{T})J_\mathrm{g} + P(\mathrm{G}^+)J_\mathrm{t} + P(\mathrm{G}^-)J_\mathrm{g} \quad (1b)$$

$$P(\mathrm{T}) + P(\mathrm{G}^+) + P(\mathrm{G}^-) = 1, \quad (1c)$$

where P(T), P(G$^+$), and P(G$^-$) are the probabilities of conformers T, G$^+$, and G$^-$ in Fig. 1 *b*, and J_t and J_g are the vicinal coupling constants between the α- and β-protons in the *trans* and *gauche* conformations, respectively. The probabilities are obtained by solving the expressions in Eq. 1. The conformers are named as above by focusing on the dihedral angle for C–C_α–C_β–C; T represents the *trans* conformer, whereas G$^+$ and G$^-$ represent the *gauche*. In G$^+$ and G$^-$, respectively, the β-CO_2^- is *trans* and *gauche* to the α-ND_3^+ (or α-ND in the peptide bond). The definition of the *trans* and *gauche* conformers of Asp within peptides corresponds to the one for Asp monomer in a previous work (Kimura et al., 2002), where the competition between the large intramolecular electrostatic energy due to α-CO_2^- and β-CO_2^- and the hydration free energy was particularly focused. In this work, we also describe the conformational equilibrium through the *trans* and *gauche* conformers with respect to C–C_α–C_β–C.

We need a parameter set of J_t and J_g to determine the conformer probabilities. The magnitude of a vicinal ^{1}H-^{1}H coupling constant for the structural unit of H-C-C-H is influenced by the electronegativities of the atoms bonded to the carbons (Glick and Bothner-By, 1956; Sheppard and Turner, 1959; Abraham and Pachler, 1963). An appropriate parameter set of J_t and J_g between α- and β-protons in amino acids was developed by Pachler (1964). Here we used Pachler's parameter set, which has been applied widely for amino acids and their residues in peptides (Bystrov, 1976). An extended-type Karplus equation, which incorporates substituent coefficients reflecting the electronegativity and the relative configuration to the coupling protons (Williams and Bhacca, 1964; Booth, 1965), has been developed by Haasnoot et al. (1980) and Altona et al. (1994). We have tested the equation to determine the probabilities of Asp monomer (Kimura et al., 2002). The probabilities estimated showed identical distribution trends with the results obtained by Pachler's parameter set, and the probability difference between the two methods was an order of 0.01. In the present work, we did not apply Altona and Haasnoot's parameters, because their parameters are not available for our peptide systems and it is desirable that the parameter set be common to all the systems treated. Feeney's set of J_t and J_g (Feeney, 1976), which also involves the substituent effects of electronegativity and configuration, led here to an estimation of some negative probabilities, so that we did not use the parameters in the present case. Thus we have adopted Pachler's set determined for amino acid and peptide systems as in our previous work (Kimura et al., 2002).

When we apply the staggered-state model to study the temperature effect on the conformational equilibrium, it should be noted that the following approximation is involved: i.e., throughout the temperature range examined, each of the staggered conformations corresponds to the probability-weighted average within the potential well. We can expect that the temperature-induced changes in the observed vicinal coupling constants mainly reflect the transfers among the potential wells rather than the shifts of the averaged conformations within the wells, since the conformational fluctuation in the well is concentrated around the potential minimum. Thus, the treatment at this level of approximation is likely to provide a good result of the temperature effect on the conformational equilibrium. Furthermore, we used Pachler's parameter set of J_t and J_g, which was evaluated at 30°C, in the conformational analyses for the different temperatures. Although a thorough determination and the application of the temperature dependence of J_t and J_g are necessary for a refinement of our results, this approximation is justified because the coupling constant at a fixed conformer is determined mainly by the electronic state and is considered weakly dependent on the temperature within 10–95°C.

The *trans*-to-*gauche* conformational free-energy change ΔG^0 was obtained from the conformational equilibrium constant K determined by the conformer probabilities. The separation of ΔG^0 into the enthalpic ΔH^0 and entropic $-T\Delta S^0$ components was done by the van't Hoff analysis. The above procedures for the conformational analysis were described in detail in the previous article (Kimura et al., 2002).

Theoretical calculations

Conformational energy change

To estimate the sequence-position dependence of the conformational energy change ΔE^0_{gas} in the gas phase (absence of solvent), we employed the structural segments involved in Asp residues at the N-, non-, and C-terminal positions: 1), CO_2^--$C_\beta H_2$-$C_\alpha H_2$-CO_2^-; 2), CO_2^--$C_\beta H_2$-$C_\alpha H_2$-CONHMe; 3), CO_2^--$C_\beta H_2$-$C_\alpha H_2$-NH_3^+; and 4), CO_2^--$C_\beta H_2$-$C_\alpha H_2$-NHCOMe were calculated by the MM2 force field (Burkert and Allinger, 1982; Schnur et al., 1991) stored in the program package of Chem 3D version 4.0 (CambridgeSoft, Cambridge, MA). The calculations separately deal with the contributions from the two pairs of vicinal groups present at each position by replacing one of the two α-groups with a hydrogen atom. Here, the α-carbon of the next residue is also replaced by a methyl group to treat the ΔE^0_{gas} of each residue in approximation independently.

ΔE^0_{gas} at each sequence position was then estimated by adding the *trans*-to-*gauche* ΔE^0_{gas} values for an appropriate pair of the segments: types 2 and 3 for the N-terminus; types 2 and 4 for the nonterminus; and types 1 and 4 for the C-terminus. At the C-terminus, for example, the β-CO_2^- interacts with both the vicinal α-CO_2^- and α-peptide bond. Therefore, the effects of the two interactions can be incorporated by adding ΔE^0_{gas} for 1 and 4 in the estimation of the C-terminal ΔE^0_{gas}. Ab initio calculations of ΔE^0_{gas} for such large systems as above are not our present target of investigation. It is expected that the difference between quantum and molecular mechanical calculations does not affect the interpretations of the hydration effect ΔG^0_{hyd} ($= \Delta G^0 - \Delta E^0_{gas}$) here, since the orders are different between the calculated ΔE^0_{gas} and experimental ΔG^0.

The dihedral angle with respect to the vicinal groups on the C_α–C_β bond was fixed in the optimization at the completely staggered *trans* or *gauche* conformer. For the segments 2 and 4, which involve the amide groups of peptide bonds, the dihedral angles N–C–C_α–C_β for 2 and C–N–C_α–C_β for 4 were varied at an interval of 10° in the optimization to estimate the range of ΔE^0_{gas}. In this estimation, the ranges of the dihedral angles corresponding to the prohibited ϕ (= H–N–C_α–C) and ψ (= O–C–C_α–N) values in the Ramachandran diagram were omitted (Ramachandran et al., 1966).

At the approximation level employed, the effect of one segment to modify ΔE^0_{gas} of the other segment is not taken into account. The effect can be evaluated by constructing a two-dimensional energy diagram with respect to the orientations of the two α-functional groups for the side-chain conformers of residue at each sequence position. The effect of interactions among the residues is not taken into account in the model calculations either. The evaluation of the above effects is a significant computational challenge and left to a subsequent work.

Conformer effective polarity

To interpret the hydration effect, the conformer effective polarity ($\mu^\dagger$) has been introduced in our previous work as an index of the strength of the solute-solvent interaction (Kimura et al., 2002). $\mu^\dagger$ is defined as the dipole moment with its coordinate origin positioned at the center of charge $\vec{r}_e = \sum_j |q_j|\vec{r}_j / \sum_j |q_j|$, and represents a degree of separation of the positive and negative partial charges within the conformer,

$$\mu^\dagger = \sum_j q_j(\vec{r}_j - \vec{r}_e) = \frac{2Q^+Q^-}{Q^+ + Q^-} l, \qquad (2)$$

where $\vec{r}_j$ is the position of a partial charge, q_j, of atom j, $2Q^+Q^-/(Q^+ + Q^-)$ is the harmonic mean of the sum of the positive charges $Q^+ = \sum_{q_j>0} q_j$ and the sum of the negative charges $Q^- = \sum_{q_j<0} |q_j|$, and l is the distance between the centers of positive and negative charges. In the case of $Q^+ = Q^-$, $\mu^\dagger$ corresponds to the conventional dipole moment μ defined for a system with no net charge. The larger the effective polarity, the stronger the interaction expected with polar water molecules. The electrostatic hydration measure, $\mu^\dagger$, is expected to be useful until the molecular level calculation becomes practical for the flexible molecules and ions in solution.

To determine how much the side-chain conformational change at each sequence position induces the effective-polarity change, $\Delta\mu^\dagger$, the value of $\mu^\dagger$ for the conformers of AspNHMe, MeCOAspNHMe, and MeCOAsp in the gas phase were calculated as the representative models of the N-, non-, and C-terminal Asp residues, respectively. In the calculations, the backbone dihedral angles ϕ and ψ were fixed at the optimized geometry for the minimum ΔE^0_{gas} of the structural segments 4 and 2, respectively. We determined $\mu^\dagger$ with the ionization states corresponding to the experimental neutral pD; the competition between the hydration and intramolecular effects is most illustrative at the neutral pD since all the ionizable groups are charged. The calculations of $\mu^\dagger$ were performed by means of the AM1 semiempirical molecular orbital calculations (Dewar et al., 1985).

RESULTS AND DISCUSSION

^{1}H NMR spectra and assignments

In this work, ^{1}H NMR were measured for a series of Asp peptides (di- to tetrapeptide) at the acidic (A), neutral (N), and basic (B) pD. The dominant ionization states of the amino and carboxyl groups at the pD values are shown in Fig. 1 *a* for the tripeptide. First, we describe the trends of ^{1}H NMR spectra at the different pDs, and assign the signals to the component amino acids from the pD effect on the chemical shifts (δ). For the tri- and tetrapeptides, the spectra are shown in Fig. 2, *a* and *b*, respectively. The carboxyl, amino, and amide protons in peptides exchange rapidly with solvent deuterons, so that the ABX-type fine structure is observed for each residue due to the coupling of one α- and two β-protons.

In the cases of peptides without ionizable side chains, such as glycine (Gly) and alanine (Ala), the ^{1}H chemical shifts of the terminal residues exhibit sensitive responses to the titration; only the chemical shifts for the N- and C-terminal residues change sensitively upon ionization of the N-terminal α-ND_2 and C-terminal α-CO_2D, respectively (Sheinblatt, 1966). In Asp peptides, all the α-proton signals move upfield upon carboxyl ionization, because Asp involves β-CO_2D in the side chain. However, the signal from the C-terminus is distinguishable in this case as well, because the magnitude of the chemical-shift change is much larger than the others due to the ionization of both α- and β-CO_2D; compare (A) and (N) in Fig. 2. Upon ionization of the ND_2, on the other hand, the marked chemical-shift change is observed only for the α-proton in the highest field, which can be assigned to the N-terminal one; compare (N) and (B) in Fig. 2.

The unassigned α-proton signals in the method above correspond to the nonterminal ones. Since the chemical shifts of the two α-protons in the tetrapeptide show similar pD dependence, they are not identified only from the titration. We can assign them by applying the sequence-position rule of the α-proton chemical shift obtained for Gly peptides; among the nonterminal α-protons, the one for the residue next to the N-terminus is always in the lowest field regardless of the ionization state (Nakamura and Jardetzky, 1968). Thus, in the Asp tetrapeptide, the α-proton signal in the

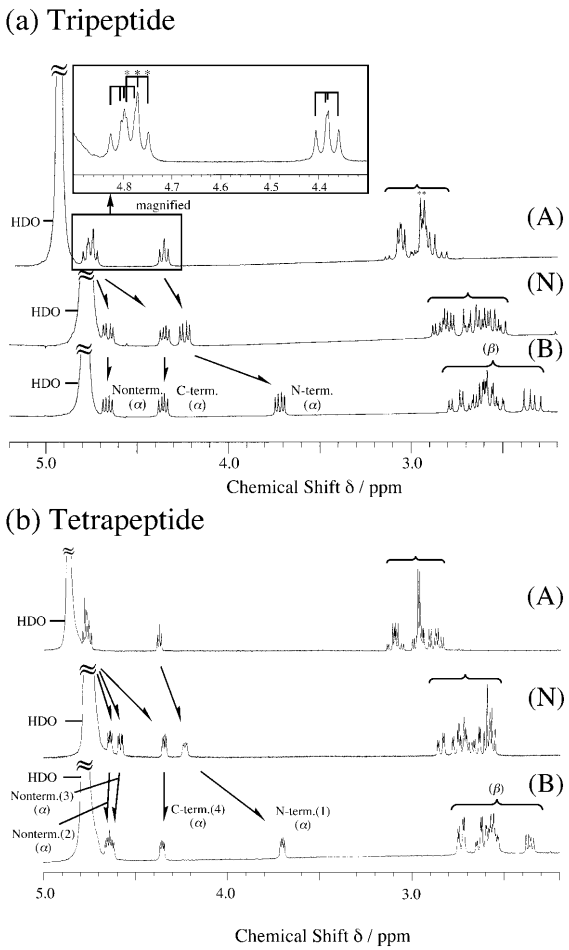

FIGURE 2 ^{1}H NMR spectrum of (*a*) 10 mM Asp tripeptide aqueous solution observed on a 270-MHz spectrometer and (*b*) 5 mM Asp tetrapeptide aqueous solution observed on a 600-MHz spectrometer at 30°C (A) at the acidic pD, (N) at the neutral pD, and (B) at the basic pD. The 5-line signals with asterisks for the tripeptide correspond to the C-terminal protons.

lowest field is assigned to the residue next to the N-terminus as shown in Fig. 2 *b*.

Unlike the α-protons, the signals of the β-protons in the Asp peptides appear without clear distinction for the component residues. We can assign them, however, by correlating to the already assigned α-protons by double-resonance measurements. Irradiation of each α-proton can be carried out without difficulty at the neutral and basic pD, because the difference in the absorption frequencies is large enough for the purpose of the double resonance.

Some signals for the tri- and tetrapeptides at the acidic pD remain unassigned because of the overlap of the α-proton signals (see *inset* in Fig. 2 *a*, for example). The overlapping signals correspond to the non- and C-terminal α-protons. We can distinguish between the non- and C-terminal signals in view of the chain-length dependence of the spectra for the peptides; for each of the di-, tri-, and tetrapeptides, only one set of the 5-line signals is observed (remember that the typical 12-line ABX-type signals change to the 5-line signals, depending on the chemical shifts and coupling constants of the three protons; Abraham and Bernstein, 1961). For the tripeptide, for example, the set of the 5-line signals is shown with asterisks in Fig. 2 *a* and consists of the strong doublet in the upfield and the triplet in the downfield. Because the number of nonterminal residues increases with the chain length, the one set of 5-line signals correspond to the C-terminus. Thus, almost all the signals at the examined pD are assigned, except for the nonterminal protons of the tetrapeptide at the acidic pD.

Finally, the assignment of the β-proton signals to the $\beta1$ and $\beta2$-protons in Fig. 1 *b* were carried out on the basis of the synthetic deuterium-labeling experiments for the Asp monomer (Kainosho and Ajisaka, 1975). Although the applicability of the assignment for the monomer to the residues in peptides is not guaranteed, it is known for most cases that the assignment can be done correctly in aqueous solution (Kobayashi et al., 1979, 1980, 1981, 1984; Cowburn et al., 1983). We assume the appropriateness of this assignment method in the present case as well.

Conformational equilibria

In this section, the sequence-position dependence of the Asp side-chain conformational equilibrium in the peptides is presented for the different ionization states of the carboxyl and amino groups.

^{1}H-^{1}H coupling constants

Table 1 summarizes the observed vicinal and geminal ^{1}H-^{1}H coupling constants among the one α- and two β-protons ($J_{\alpha\beta1}$, $J_{\alpha\beta2}$, and $J_{\beta1\beta2}$) of the Asp residues at the acidic, neutral, and basic pD values. The coupling constants for Asp amino acid monomer obtained in our previous work (Kimura et al., 2002) are shown together. At any sequence position, the difference between the vicinal $J_{\alpha\beta1}$ and $J_{\alpha\beta2}$ is larger when the carboxyl groups are ionized at the neutral and basic pD values. The larger difference means a more inclined conformer distribution. In other words, the carboxyl ionization induces a more inclined distribution at any position. The ionization effect of the amino group on $J_{\alpha\beta1}$ and $J_{\alpha\beta2}$ is less significant even at the N-terminus, where the amino group is directly bonded.

Conformer probabilities

According to $J_{\alpha\beta1}$ and $J_{\alpha\beta2}$ in Table 1, we determined the probabilities P(T), $P(G^+)$, and $P(G^-)$ of side-chain conformers T, G^+, and G^- in Fig. 1 *b*, respectively. The P(T), $P(G^+)$, and $P(G^-)$ values are illustrated in Fig. 3. Comparison of the acidic (A) and neutral (N) pD values shows that the conformer probabilities are changed by ~0.25 upon carboxyl

TABLE 1 Observed spin-spin coupling constants (Hz) among the α- and β-protons of Asp amino acid monomers and peptides (di- to tetrapeptide) at the acidic, neutral, and basic pD values

pD	J	Amino acid monomer*	Dipeptide		Tripeptide		Tetrapeptide			
			N-term.	C-term.	N-term.	Nonterm.	C-term.	N-term. (1)	Nonterm. (2)	Nonterm. (3)	C-term. (4)
Acidic	$J_{\alpha\beta1}$	6.37 ± 0.05	7.68 ± 0.04	_†	7.26 ± 0.01	7.72 ± 0.01	_†	7.12 ± 0.03	7.36 ± 0.01§	7.65 ± 0.03§	_†
	$J_{\alpha\beta2}$	4.32 ± 0.05	4.85 ± 0.05	_†	5.30 ± 0.01	5.59 ± 0.03	_†	5.38 ± 0.02	5.90 ± 0.01§	5.45 ± 0.01§	_†
	$J_{\beta1\beta2}$	18.36 ± 0.01	18.13 ± 0.03	_†	18.03 ± 0.00	17.18 ± 0.01	_†	18.04 ± 0.01	17.33 ± 0.04§	16.92 ± 0.05§	_†
Neutral	$J_{\alpha\beta1}$	9.10 ± 0.01	10.40 ± 0.00	10.44 ± 0.00	10.34 ± 0.01	10.31 ± 0.01	8.79 ± 0.02	9.96 ± 0.07	8.77 ± 0.03	10.31 ± 0.00	8.98 ± 0.01
	$J_{\alpha\beta2}$	3.58 ± 0.02	3.86 ± 0.00	3.63 ± 0.00	3.93 ± 0.02	4.09 ± 0.04	4.05 ± 0.02	4.16 ± 0.02	4.52 ± 0.03	3.92 ± 0.05	4.09 ± 0.05
	$J_{\beta1\beta2}$	17.47 ± 0.01	17.38 ± 0.01	15.64 ± 0.01	17.36 ± 0.01	15.99 ± 0.03	15.58 ± 0.01	17.29 ± 0.02	16.14 ± 0.05	16.10 ± 0.02	15.95 ± 0.02
Basic	$J_{\alpha\beta1}$	10.08 ± 0.00	9.76 ± 0.00	9.15 ± 0.01	9.24 ± 0.01	9.26 ± 0.01	8.77 ± 0.00	8.79 ± 0.02	8.62 ± 0.02¶	9.12 ± 0.02¶	8.69 ± 0.02¶
	$J_{\alpha\beta2}$	3.64 ± 0.01	3.94 ± 0.01	4.09 ± 0.01	4.37 ± 0.01	4.46 ± 0.00	4.39 ± 0.01	4.63 ± 0.02	4.92 ± 0.02¶	5.02 ± 0.02¶	4.47 ± 0.02¶
	$J_{\beta1\beta2}$	15.30 ± 0.00	15.58 ± 0.01	15.54 ± 0.00	15.62 ± 0.00	15.93 ± 0.00	15.67 ± 0.01	15.61 ± 0.02	16.03 ± 0.02¶	16.10 ± 0.02	15.78 ± 0.02¶

*Taken from Kimura et al. (2002).
†Values could not be determined due to the 5-line signals.
§Assignment for these nonterminal residues may be opposite.
¶Values including uncertainties because of signal overlap.

ionization. *Trans* conformer T becomes more favorable. This response is in accordance with the *trans* preference observed for Asp in various peptides at neutral pD (Feeney et al., 1972; Bartle et al., 1972; Ishii et al., 1985). Upon amino ionization, the conformer probabilities do not change as drastically, at $\leq\sim0.10$.

Sequence-position dependence

When the carboxyl groups are not ionized at the acidic pD, the sequence-position dependence of the conformer distribution is small; the probability differences among the positions are only ≤0.08. The distributions for the peptides exhibit a different trend from that for the monomer; conformer T is the most probable in the peptides, whereas G^- is in the monomer. At any position in peptides, however, there is a common trend to the monomer case that the conformer distribution at the acidic pD is less inclined than that at the neutral or basic pD.

Upon ionization of the carboxyl groups, the conformer distributions become more inclined, while the small position dependence remains as it is before the ionization. This observation is of particular interest, in view that the carboxyl ionization is expected to induce a substantial position dependence of the intramolecular electrostatic interaction energy. To estimate the position dependence of the intramolecular effect, the *trans*-to-*gauche* conformational energy changes of ΔE^0_{gas} in the gas phase (absence of solvent) were calculated by the MM2 for the structural segments (1–4) in Fig. 4 involving a pair of vicinal groups present in the Asp residues.

Fig. 4 diagrammatically presents the ΔE^0_{gas} values. For the cases 2 and 4 including the amide groups of peptide bonds, ΔE^0_{gas} is given not only for the minimum values but also for the maximum ones to show the orientation effect of the amide group (see the minimum values as the stable geometry). ΔE^0_{gas} is of order of tens of kJ mol^{-1} and depends strongly on the segment structure. By adding the ΔE^0_{gas} values in Fig. 4, the position dependence of $\Delta E^0_{gas}(T\rightarrow G^+,G^-)$ can be estimated as shown in Fig. 5. Here the N-terminus involves the segment types 2 and 3, the nonterminus involves 2 and 4, and the C-terminus involves 1 and 4.

$E^0_{gas}(T\rightarrow G^+,G^-)$ at each sequence position is of tens of kJ mol^{-1} except for the nonterminal $T\rightarrow G^+$. In contrast, the free energy change $\Delta G^0(T\rightarrow G^+,G^-)$ obtained experimentally by the conformer distribution has a magnitude of a few kJ mol^{-1}. Hence, the hydration effect ΔG^0_{hyd} ($=\Delta G^0-\Delta E^0_{gas}$) almost cancels the enormous intramolecular electrostatic effect ΔE^0_{gas}. This is common to the observation for Asp monomer. Furthermore, ΔE^0_{gas} exhibits a marked position dependence by tens of kJ mol^{-1}. The position dependence of experimental ΔG^0 is much weaker with 1–2 kJ mol^{-1}. It can be thus concluded that the hydration also compensates for the position dependence of the intramolecular interactions.

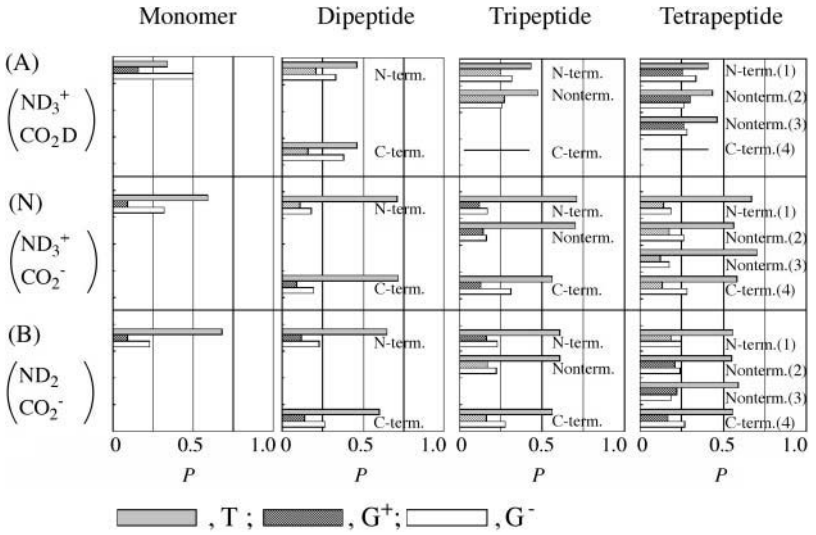

FIGURE 3 Probabilities (P) of side-chain conformers T, G^+, and G^- in Fig. 1 *b* for the Asp amino acid monomer and peptides (di-, tri-, and tetrapeptides) (A) at the acidic pD, (N) at the neutral pD, and (B) at the basic pD.

The ionic side chain of Asp can occupy both the staggered *trans* and *gauche* conformers on the C_α-C_β bond at every N-, non-, and C-terminal position, because of the presence of water solvent. In the absence of hydration, on the contrary, the Asp residues can only take a single conformer at a physiological temperature of $RT = \sim 2.6$ kJ mol^{-1}.

Compared to the effect of the carboxyl ionization, that of the amino ionization on the conformational equilibria is smaller even at the N-terminus in peptides or amino acid monomer, where the amino group is directly bonded. To be more precise, the distribution between T and G^- becomes more inclined by the amino ionization for the N-terminus of the peptides and becomes less inclined for the monomer. Note that the β-CO_2^- is *gauche* to the α-ND_3^+/ND_2 in both T and G^-. The probability of conformer G^+ is scarcely affected upon the ionization. Thus, the electrostatic attraction between the vicinal β-CO_2^- and α-ND_3^+ is not the dominant controlling factor of the equilibrium, because the probability change induced by the amino ionization is mostly the rearrangement between the conformers *gauche* with respect to the CO_2^- and ND_3^+(ND_2) but not between the conformers *trans* and *gauche*. This conclusion is in accordance with the observations that the conformer distribution on the alkyl C-C bond of β-alanine (NH_3^+-CH_2-CH_2-COO^-) in aqueous solution is scarcely affected upon ionization of the carboxyl and amino groups (Gregoire et al., 1998). The changes in the conformer distribution upon amino ionization shows again that the hydration effect compensates for the large intramolecular electrostatic effect due to ionic groups.

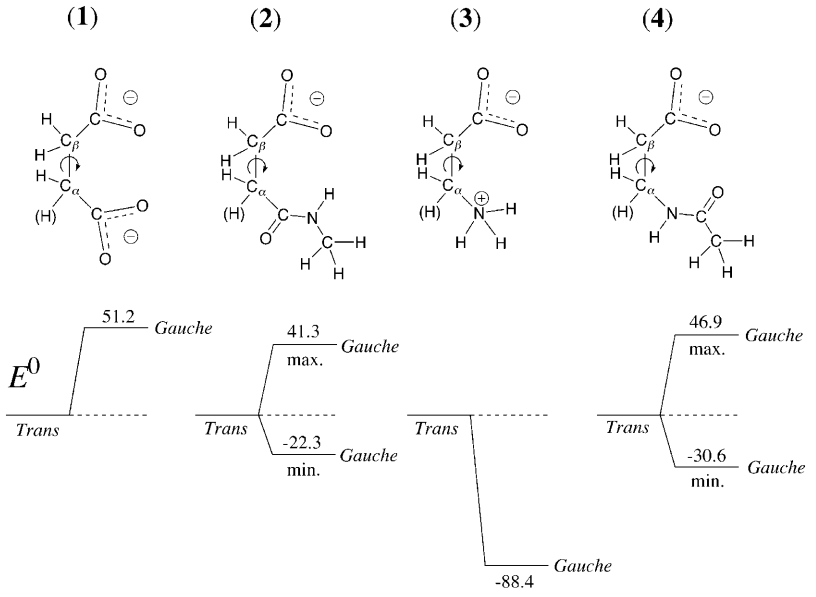

FIGURE 4 Conformational energy changes ΔE^0_{gas} (kJ mol^{-1}) in the gas phase calculated by the MM2 for the *trans*-to-*gauche* transformation with respect to a pair of vicinal functional groups involved in Asp residues in peptides. One α-functional group was replaced by a hydrogen atom in the calculations as shown in the parentheses. In the cases where the α-amide group of a peptide bond is involved as for 2 and 4, not only the minimum but also the maximum values of ΔE^0_{gas} due to the variation of the orientation of this group are shown.

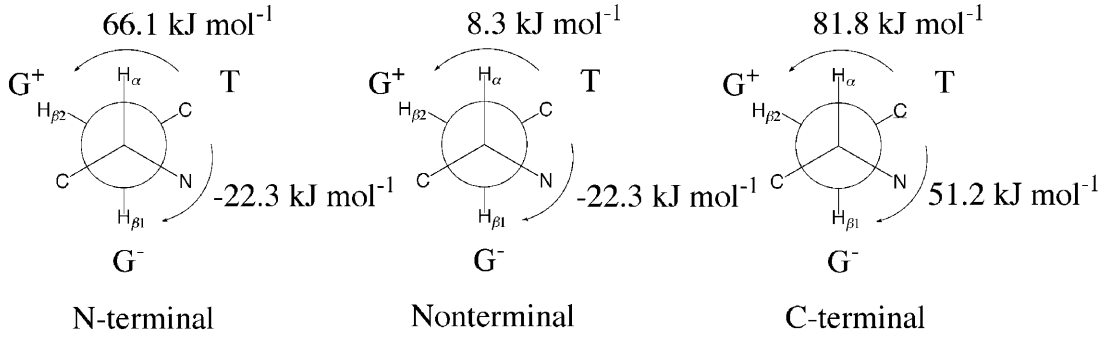

FIGURE 5 Sequence-position dependence of the conformational energy changes ΔE^0_{gas} (kJ mol^{-1}) in the gas phase.

Hydration effect and effective polarity

In this section, we interpret the hydration effect from the degree of separation of positive and negative partial charges within the conformers. In the previous work (Kimura et al., 2002), a correlation was observed for Asp monomer between the conformational changes in the hydration free energy and in the effective polarity $\mu^\dagger$. The larger $\mu^\dagger$ causes stronger electrostatic hydration, which further stabilizes the conformer. Here we calculated $\mu^\dagger$ for the conformers of AspNHMe, MeCOAspNHMe, and MeCOAsp in the gas phase as representative models of the N-, non-, and C-terminal Asp residues, respectively. The ionization states in the calculations correspond to the experimental neutral pD; the connection of $\mu^\dagger$ to the hydration effect is most illustrative at the neutral pD. Table 2 summarizes the results.

At the N-terminus, the side-chain β-CO_2^- is strongly attracted intramolecularly by both the vicinal α-ND_3^+ and α-COND as seen in Fig. 4. Since the attractive interaction is even stronger for α-ND_3^+ than for α-COND, the order of conformer preference due solely to the intramolecular effect is $G^- \gg T \gg G^+$. Accordingly, the observed comparable probabilities among the conformers in Fig. 3 indicate that the hydration stabilizes the conformers in the opposite order to the intramolecular effect. The order of effective polarity is $\mu^\dagger(G^+) > \mu^\dagger(T) > \mu^\dagger(G^-)$, and is thus in accordance with the order of the hydration effect. In other words, the hydration effect can be qualitatively interpreted through $\mu^\dagger$, and $\mu^\dagger$ may be considered as an index of the strength of solute-solvent interactions. At the C-terminus, the order of preference due solely to the intramolecular effect is estimated to be $T \gg G^- \gg G^+$. The order of effective polarity is opposite—$\mu^\dagger(G^+) > \mu^\dagger(G^-) > \mu^\dagger(T)$. Thus, the hydration effect at the C-terminus also reflects $\mu^\dagger$ in a qualitative manner. At the nonterminus, however, the hydration effect is in the order of $G^+ > T > G^-$ and does not agree with the $\mu^\dagger$ order. Actually, the hydration is sterically more restricted at the nonterminal residues than at the terminal residues. Due to the presence of the neighboring residues on both sides of the primary sequence, the hydration at the nonterminal residues does not simply reflect $\mu^\dagger$.

TABLE 2 Effective polarities $\mu^\dagger$ (D) of Asp side-chain conformers T, G^+, and G^- in Fig. 1 *b* at the ionization state of neutral pD

Conformer	Amino acid monomer*	Peptide		
		N-terminal†	Nonterminal‡	C-terminal§
T	7.1	11.8	13.7	8.6
G^+	–¶	12.3	9.7	14.1
G^-	11.2	10.8	10.9	11.4

Values determined by the AM1 except for the monomer by the ab initio method. Note that the superscript † on μ is not for the footnote.
*Taken from Kimura et al. (2002).
†For Asp-NHMe.
‡For MeCO-Asp-NHMe.
§For MeCO-Asp.
¶Value could not be obtained due to the hydrogen transfer from α-NH_3^+ to α-CO_2^- in the optimization.

Conformational free energy and the enthalpic and entropic components

In this section, we focus on the thermodynamics accompanying the conformational change to gain further insight into the sequence-position dependence of the conformational equilibrium. We investigate *trans*-to-*gauche* ΔG^0 and its enthalpic ΔH^0 and entropic $-T\Delta S^0$ components. Before going to the Discussion, we first see the observed temperature effect on the vicinal coupling constants. The examination of the temperature effect for the separation of ΔH^0 and $-T\Delta S^0$ was done at acidic and neutral pD values, focusing on the marked ionization effect of the carboxyl groups on the conformational equilibria.

Temperature dependence of vicinal J

Table 3 summarizes the ^{1}H-^{1}H coupling constants J for Asp dipeptide at the acidic (A) and neutral (N) pD in the temperature range of 10 to 90°C. The difference between the vicinal constants $J_{\alpha\beta1}$ and $J_{\alpha\beta2}$ gets slightly smaller with the temperature increase at both the N- and C-terminal positions. For Asp tri- and tetrapeptides, the difference between $J_{\alpha\beta1}$ and $J_{\alpha\beta2}$ also shows a similar trend with temperature at the N-, non-, and C-terminal positions at both acidic and neutral

TABLE 3 Observed spin-spin coupling constants (Hz) among the α- and β-protons of Asp residues in the dipeptide at the acidic and neutral pD at various temperatures

pD	Residue	J	Temperature/°C								
			10	20	30 (neutral) 25 (acidic)	40	50	60	70	80	90
Acidic (pD = 0.6)	N-terminal	$J_{\alpha\beta1}$	7.84 ± 0.09	7.76 ± 0.06	7.68 ± 0.04	7.46 ± 0.00	7.39 ± 0.02	7.40 ± 0.04	7.49 ± 0.01*	7.32 ± 0.02	7.30 ± 0.04
		$J_{\alpha\beta2}$	4.73 ± 0.04	4.85 ± 0.05	4.85 ± 0.05	5.00 ± 0.02	5.07 ± 0.01	5.07 ± 0.02	5.27 ± 0.02*	5.15 ± 0.02	5.17 ± 0.03
		$J_{\beta1\beta2}$	18.20 ± 0.04	18.15 ± 0.03	18.13 ± 0.03	18.05 ± 0.04	18.04 ± 0.01	18.00 ± 0.03	18.00 ± 0.03	17.98 ± 0.02	17.97 ± 0.01
	C-terminal	$J_{\alpha\beta1}$	†‡	†‡	†‡	†‡	‡	7.34 ± 0.08	7.24 ± 0.04	7.10 ± 0.04	7.06 ± 0.02
		$J_{\alpha\beta2}$	†‡	†‡	†‡	†‡	‡	4.70 ± 0.06	4.84 ± 0.04	5.00 ± 0.04	5.09 ± 0.03
		$J_{\beta1\beta2}$	†‡	†‡	†‡	†‡	17.40 ± 0.14	17.27 ± 0.05	17.20 ± 0.01	17.14 ± 0.01	17.11 ± 0.01
Neutral (pD = 7.4)	N-terminal	$J_{\alpha\beta1}$	10.49 ± 0.02	10.42 ± 0.01	10.40 ± 0.00	10.37 ± 0.01	10.34 ± 0.01	10.28 ± 0.01	10.23 ± 0.01	10.17 ± 0.01	10.14 ± 0.01
		$J_{\alpha\beta2}$	3.76 ± 0.01	3.83 ± 0.01	3.86 ± 0.00	3.90 ± 0.01	3.91 ± 0.01	3.95 ± 0.01	3.99 ± 0.01	4.01 ± 0.01	4.02 ± 0.01
		$J_{\beta1\beta2}$	17.46 ± 0.02	17.41 ± 0.02	17.38 ± 0.01	17.35 ± 0.00	17.32 ± 0.01	17.26 ± 0.01	17.20 ± 0.01	17.15 ± 0.00	17.10 ± 0.01
	C-terminal	$J_{\alpha\beta1}$	10.77 ± 0.00	10.58 ± 0.01	10.44 ± 0.00	10.32 ± 0.00	10.11 ± 0.02	9.99 ± 0.01	9.80 ± 0.01	9.63 ± 0.01	9.49 ± 0.01
		$J_{\alpha\beta2}$	3.48 ± 0.03	3.56 ± 0.01	3.63 ± 0.00	3.78 ± 0.00	3.87 ± 0.03	3.94 ± 0.01	3.96 ± 0.02	4.00 ± 0.02	4.08 ± 0.01
		$J_{\beta1\beta2}$	15.72 ± 0.02	15.68 ± 0.01	15.64 ± 0.01	15.61 ± 0.01	15.56 ± 0.00	15.51 ± 0.00	15.47 ± 0.00	15.42 ± 0.01	15.39 ± 0.00

*Values including uncertainties because of signal overlap.
†Values could not be obtained because of the 5-line signals.
‡Values could not be obtained because of signal overlap.

pD values. The only case in which we were not able to identify the similar trend is the C-terminus at the acidic pD, where the vicinal J could not be obtained due to the 5-line signals (Abraham and Bernstein, 1961) or to the fast breaking of the peptide bonds. The decrease in the difference between $J_{\alpha\beta1}$ and $J_{\alpha\beta2}$ means the more even conformer probabilities at higher temperatures.

ΔG^0, ΔH^0, and $-T\Delta S$

According to the conformer probabilities $P(\mathrm{T})$, $P(\mathrm{G}^+)$, and $P(\mathrm{G}^-)$ determined from $J_{\alpha\beta1}$ and $J_{\alpha\beta2}$, the *trans-gauche* conformational equilibrium constant $K = P(\mathrm{G}^+,\mathrm{G}^-)/P(\mathrm{T})$ is obtained. The van't Hoff plots of ln K are shown in Fig. 6, *a* and *b*, for the dipeptide (corresponding data for the tri- and tetrapeptides are provided in Supplementary Material). The plots are linear, and ΔH^0 is temperature-independent. Temperature independence of ΔH^0 was common to the tri- and tetrapeptides. The obtained $\Delta G^0(\mathrm{T}\rightarrow\mathrm{G}^+,\mathrm{G}^-)$, $\Delta H^0(\mathrm{T}\rightarrow\mathrm{G}^+,\mathrm{G}^-)$, and $-T\Delta S^0(\mathrm{T}\rightarrow\mathrm{G}^+,\mathrm{G}^-)$ at the N-, non-, and C-terminal positions of di- to tetrapeptides at 30°C are summarized in Table 4. The thermodynamic quantities for

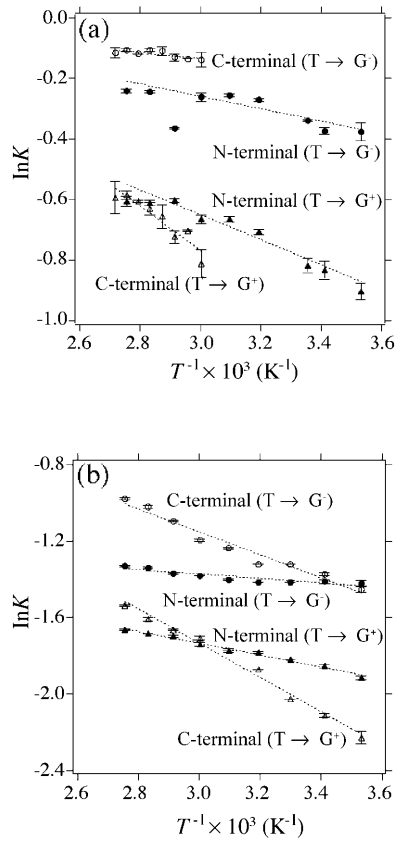

FIGURE 6 ln K against $1/T$ for the Asp side-chain conformational equilibria in Asp dipeptide. $K = P(\mathrm{x})/P(\mathrm{T})$ is the equilibrium constant, where $P(\mathrm{T})$ is the probability of conformer T, and $P(\mathrm{x})$ is the probability of conformer G^+ or G^-. T is the absolute temperature. (*a*) At the acidic pD of 0.6 and (*b*) at the neutral pD of 7.4.

TABLE 4 Changes in the standard free energy ΔG^0, enthalpy ΔH^0, and entropy $-T\Delta S^0$ (kJ mol^{-1}) accompanying the Asp side-chain conformational variations in amino acid monomer and in residues at peptide N-, non-, and C-terminal positions

				Peptide†							
		Amino acid monomer*		N-terminal		Nonterminal (2)		Nonterminal (3)		C-terminal	
pD		T→G$^+$	T→G$^-$	T→G$^+$	T→G$^-$	T→G$^+$	T→G$^-$	T→G$^+$	T→G$^-$	T→G$^+$	T→G$^-$
Acidic	ΔG^0	2.0 ± 0.1	−1.0 ± 0.1	1.2 ± 0.1	0.5 ± 0.0	0.9 ± 0.0	1.2 ± 0.1	1.4 ± 0.1	1.3 ± 0.1	–‡	–‡
				1.4 ± 0.0	0.7 ± 0.1	1.4 ± 0.1	1.5 ± 0.0			–‡	–‡
				2.0 ± 0.1	0.8 ± 0.1					2.7 ± 0.1	0.4 ± 0.1
	ΔH^0	1.0 ± 0.3	−2.8 ± 0.0	−0.2 ± 0.4	0.9 ± 1.0	0.0 ± 0.8	2.6 ± 0.7	3.9 ± 0.6	1.1 ± 0.7	–‡	–‡
				0.5 ± 0.2	0.3 ± 0.1	1.6 ± 0.4	1.7 ± 0.2			–‡	–‡
				3.2 ± 0.3	1.6 ± 0.5					6.1 ± 0.2	0.9 ± 0.1
	$-T\Delta S^0$	1.0 ± 0.4	1.8 ± 0.1	1.4 ± 0.5	−0.4 ± 1.0	0.9 ± 0.8	−1.4 ± 0.8	−2.5 ± 0.7	0.2 ± 0.8	–‡	–‡
				0.9 ± 0.2	0.4 ± 0.2	−0.2 ± 0.5	−0.2 ± 0.2			–‡	–‡
				−1.2 ± 0.4	−0.8 ± 0.6					−3.4 ± 0.3	−0.5 ± 0.2
Neutral	ΔG^0	4.8 ± 0.0	1.6 ± 0.0	3.9 ± 0.1	3.2 ± 0.1	2.9 ± 0.1	1.9 ± 0.0	4.5 ± 0.1	3.5 ± 0.1	3.7 ± 0.1	1.8 ± 0.1
				4.4 ± 0.1	3.5 ± 0.1	4.1 ± 0.1	3.7 ± 0.1			3.7 ± 0.1	1.6 ± 0.0
				4.6 ± 0.0	3.6 ± 0.0					5.1 ± 0.0	3.3 ± 0.0
	ΔH^0	1.7 ± 0.2	−1.9 ± 0.1	0.4 ± 0.2	−0.2 ± 0.4	4.9 ± 0.4	3.1 ± 0.8	4.9 ± 0.4	2.5 ± 0.3	9.9 ± 0.3	4.1 ± 0.0
				2.8 ± 0.5	1.7 ± 0.8	1.4 ± 1.0	3.9 ± 1.5			1.8 ± 3.6	8.9 ± 1.6
				2.6 ± 0.1	1.0 ± 0.2					7.4 ± 0.2	5.0 ± 0.1
	$-T\Delta S^0$	3.1 ± 0.2	3.5 ± 0.1	3.5 ± 0.3	3.4 ± 0.5	−2.0 ± 0.5	−1.2 ± 0.8	−0.4 ± 0.5	1.0 ± 0.4	−6.2 ± 0.4	−2.3 ± 0.1
				1.6 ± 0.6	1.8 ± 0.9	2.7 ± 1.1	−0.2 ± 1.6			1.9 ± 3.7	−7.3 ± 1.6
				2.0 ± 0.1	2.6 ± 0.2					−2.3 ± 0.2	−1.7 ± 0.1

ΔG^0 and $-T\Delta S^0$ correspond to the values at 30°C except for the dipeptide acidic solution at 25°C. The temperature difference between 25 and 30°C affects the ΔG^0 and $-T\Delta S^0$ values by ≤0.1 kJ mol^{-1}. ΔH^0 is temperature-independent in the measured range.

*Taken from Kimura et al. (2002).

†Values in the top, middle, and bottom lines for each of the thermodynamic quantities are from the tetra-, tri-, and dipeptides, respectively.

‡Values could not be obtained because of the 5-line signals at low temperatures and of the fast breaking of peptide bonds at high temperatures.

the amino acid monomer (Kimura et al., 2002) are listed together in the table.

ΔG^0, ΔH^0, and $-T\Delta S^0$ in Table 4 are illustrated in Fig. 7. As referred to above, almost all ΔG^0 at the neutral pD are smaller than the corresponding ΔE^0_{gas} in the absolute value by one order of magnitude, and thus the hydration free energy ΔG^0_{hyd} (= ΔG^0–ΔE^0_{gas}) competes against the large intramolecular effect ΔE^0_{gas}. The enthalpic component ΔH^0 at the neutral pD has the magnitude of the same order as ΔG^0. Therefore, the competing effect of the hydration ΔG^0_{hyd} is mainly due to the hydration enthalpy ΔH^0_{hyd} (= ΔH^0–ΔE^0_{gas}). This observation is common to the case for the Asp monomer (Kimura et al., 2002).

Most of the entropic components $-T\Delta S^0$ are larger at the neutral pD than at the acidic. Since $-T\Delta S^0$ in aqueous solution is dominated by the hydration effect $-T\Delta S^0_{hyd}$, the difference in the electrostatic hydration between the *trans* and *gauche* conformers is more distinct when the carboxyl groups are ionized at the neutral pD. This trend of $-T\Delta S^0_{hyd}$ is attributed to the presence of the full-charged groups and the larger conformational changes in the charge distribution at the neutral pD.

The position dependence of ΔG^0(T→G$^+$,G$^-$) is small within ~1–2 kJ mol^{-1} even when the carboxyl groups are ionized. In contrast to ΔG^0, its components ΔH^0(T→G$^+$,G$^-$) and $-T\Delta S^0$(T→G$^+$,G$^-$) exhibit notable trends at the C-terminus. At the neutral pD, except for T→G$^+$ in the tripeptide, the C-terminal ΔH^0 is larger than the N- and non-terminal ones, and the corresponding $-T\Delta S^0$ is smaller to be negative. The larger ΔH^0 is attributed to the strong intramolecular electrostatic repulsion between α-CO_2^- and β-CO_2^- present at the C-terminus (see Fig. 5). The negative $-T\Delta S^0$ means that the solute-solvent interaction at the C-terminus serves as a structure-breaker for the solvent.

Since both the peptide C-terminus and monomer involve α-CO_2^- and β-CO_2^-, it is of particular interest to compare their ΔH^0(T→G$^+$,G$^-$) in connection to the hydration effect ΔH^0_{hyd}(T→G$^+$,G$^-$). In Fig. 7, ΔH^0 is obviously larger for the peptide C-terminus except for T→G$^+$ in the tripeptide. The larger ΔH^0 indicates that the hydration enthalpy ΔH^0_{hyd} competes less against the strong repulsion energy ΔE^0_{gas} between α-CO_2^- and β-CO_2^-. This phenomenon is attributed to the presence of neighbor residues. The C-terminal Asp is less surrounded by hydrating water molecules than the monomer, so that the hydration effect that reduces the enthalpies of the *gauche* conformers G$^+$ and G$^-$ is expected to be weaker at the C-terminus.

Asp in Achatin-I peptide

In this section, we investigate the conformational equilibrium of Asp side chain in achatin-I (Gly-D-Phe-Ala-Asp). In achatin-I, the residue next to the C-terminal Asp is not Asp but alanine (Ala). The effect of the absence of ionic groups in the sequence neighbor is thus of interest. We examine

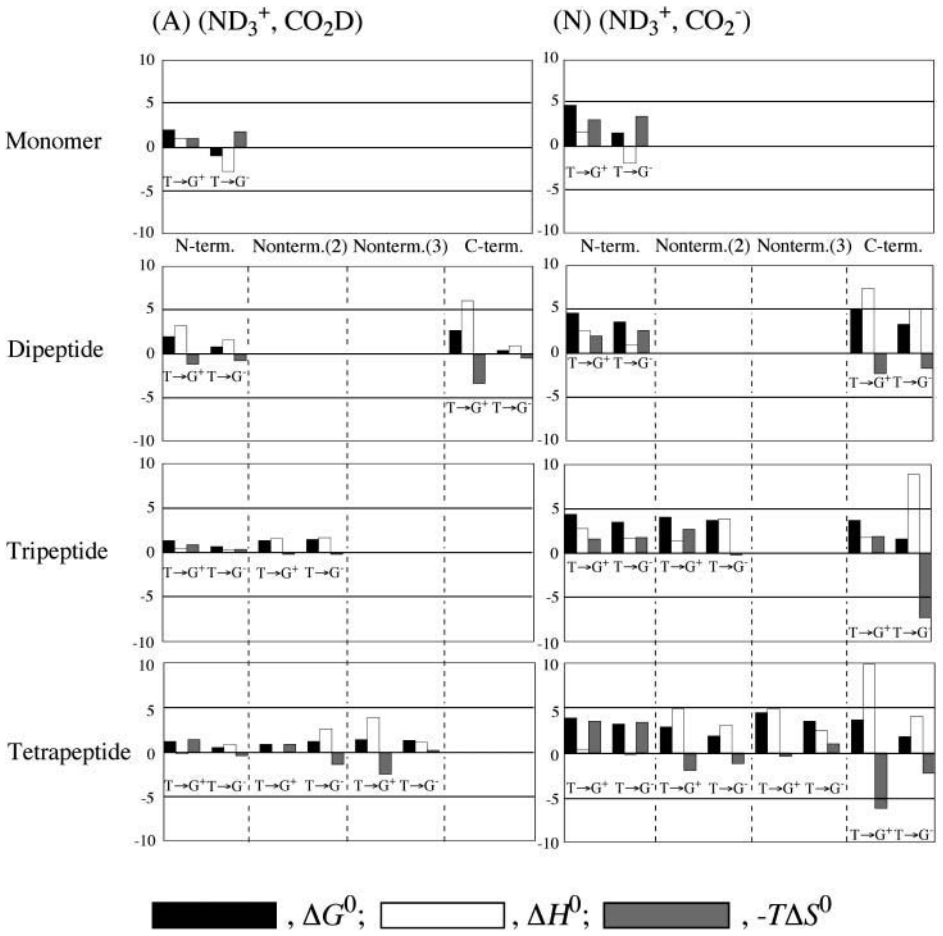

FIGURE 7 Side-chain conformational changes in the standard free energy ΔG^0, enthalpy ΔH^0, and entropy $-T\Delta S^0$ (kJ mol^{-1}) from T to G^+ or G^- in Fig. 1 *b* of Asp amino acid monomer, di-, tri-, and tetrapeptides (A) at the acidic pD and (N) at the neutral pD.

whether or not the thermodynamic trend is common between the C-terminal Asp in the model peptides and in achatin-I.

Fig. 8 shows the ^{1}H NMR spectra at the acidic (A), neutral (N), and basic (B) pD values. As seen in the figure, the proton signals from the four component amino acid residues are well separated at any pD. The signals of the α- and β-protons in the C-terminal Asp can be easily identified; they move upfield in response to the ionization of carboxyl groups

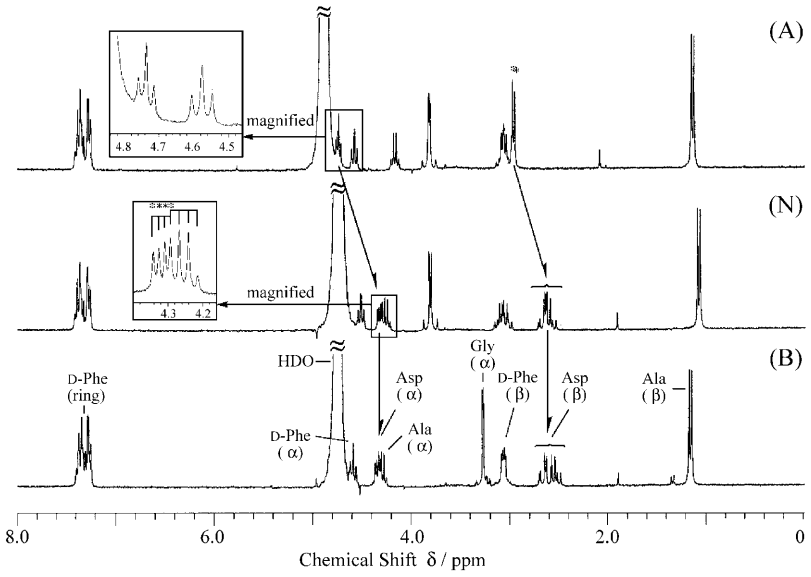

FIGURE 8 ^{1}H NMR spectrum of 2 mM achatin-I (Gly-D-Phe-Ala-Asp) aqueous solution at 30°C (A) at the acidic pD of 0.7, (N) at the neutral pD of 7.5, and (B) at the basic pD of 13.8.

as indicated by an arrow. In accordance with the observations for the Asp peptides, the C-terminal Asp in achatin-I shows at room temperature the 5-line signals at the acidic pD and the typical 12-line signals at the neutral and basic pD values.

The vicinal $J_{\alpha\beta1}$ and $J_{\alpha\beta2}$ can be determined from the 12-line signals at the neutral and basic pD values, whereas $J_{\alpha\beta1}$ and $J_{\alpha\beta2}$ cannot be determined at the acidic pD due to the 5-line signals (Abraham and Bernstein, 1961). It was found, however, that the signal type at the acidic pD changes from 5- to 12-line at higher temperatures over ~60°C. Thus we can determine $J_{\alpha\beta1}$ and $J_{\alpha\beta2}$ at every pD by the analysis of the ABX-type signals.

The conformer distributions obtained by the analysis of $J_{\alpha\beta1}$ and $J_{\alpha\beta2}$ at the acidic (60°C), neutral (30°C), and basic (30°C) pD are shown in Fig. 9. The probability of *trans* conformer T is increased upon ionization of the carboxyl groups. This trend of ionization effect is the same as that for the C-terminal Asp in the Asp peptide described in the above section. The probabilities are similar for the C-terminal Asp residue in achatin-I and in Asp peptides at any pD with the difference of 0.04 to 0.10 (compare Figs. 3 and 9).

The van't Hoff plots of ln K at the neutral pD are shown in Fig. 10. The plots are linear, and ΔG^0(T→G$^+$,G$^-$), ΔH^0(T→G$^+$,G$^-$), and $-T\Delta S^0$(T→G$^+$,G$^-$) obtained at 30°C are summarized in Table 5. As characteristically observed for Asp peptides, the ΔH^0 of the C-terminal Asp in achatin-I has a large positive value and the corresponding $-T\Delta S^0$ has a large negative value, compared to those of the N- and nonterminal Asp. The replacement of the ionic neighbor residues by the hydrophobic ones such as Ala and phenylalanine (Phe) does not affect ΔG^0, ΔH^0, and $-T\Delta S^0$ drastically at the C-terminal Asp. Thus, the C-terminal trend of the conformational equilibrium obtained for Asp in achatin-I is confirmed to be similar to the trend observed in the model Asp peptides. If we apply the ΔE^0_{gas} values in Fig. 5, the signs of the hydration enthalpy ΔH^0_{hyd} (= ΔH^0–ΔE^0_{gas}) and the hydration entropy $-T\Delta S^0_{hyd}$ (= $-T\Delta S^0$) are obtained to be negative. The negative ΔH^0_{hyd} and $-T\Delta S^0_{hyd}$ indicate that the hydration effect drives both enthalpically and entropically the Asp side chain to the *gauche* conformers G$^+$ and G$^-$, which are unstable without hydration.

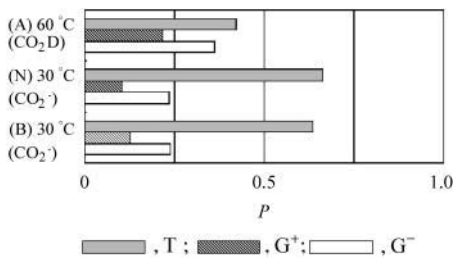

FIGURE 9 Probabilities (P) of side-chain conformers T, G$^+$, and G$^-$ in Fig. 1 *b* for the C-terminal Asp in achatin-I, (A) at the acidic pD, (N) at the neutral pD, and (B) at the basic pD.

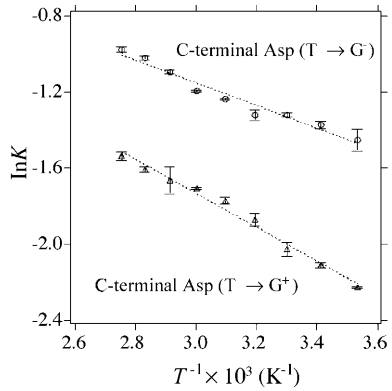

FIGURE 10 ln K against 1/T for the C-terminal Asp in achatin-I at the neutral pD.

CONCLUSIONS

We investigated the sequence-position dependence of side-chain conformational thermodynamics for Asp residue in a series of model peptides (Asp di- to tetra) and achatin-I (Gly-D-Phe-Ala-Asp) in aqueous solution. *Trans*-to-*gauche* ΔG^0, ΔH^0, and $-T\Delta S^0$ were obtained with respect to the dihedral angle of C–C$_\alpha$–C$_\beta$–C by measuring the temperature dependence of the vicinal couplings in NMR.

The position dependence of ΔG^0 is small within ~1–2 kJ mol^{-1} even when the carboxyl groups are ionized at neutral pH. On the other hand, the conformational changes in the intramolecular energy ΔE^0_{gas} in the gas phase depend on the position by tens of kJ mol^{-1}. Therefore, the small position-dependence of ΔG^0 is a result of the compensating effect of hydration. The hydration effect ΔG^0_{hyd} (= ΔG^0–ΔE^0_{gas}) mostly reflects the enthalpic contribution ΔH^0_{hyd} and is correlated with the degree of separation of positive and negative partial charges within the conformer at the terminal positions, which are well exposed to the solvent compared to the nontermini.

In contrast to the sequence-position dependence of ΔG^0, the enthalpic ΔH^0 and entropic $-T\Delta S^0$ components exhibit a notable trend at the C-terminus; the C-terminal ΔH^0 is larger than those at the N- and nontermini and the C-terminal $-T\Delta S^0$ is negative and larger in magnitude than the others. The larger ΔH^0 at the C-terminus is due to the strong intramolecular repulsion between α-CO$_2^-$ and β-CO$_2^-$. The negative $-T\Delta S^0$ means that the solute-solvent interaction serves as a structure breaker of the water solvent.

TABLE 5 Changes in the standard free energy ΔG^0, enthalpy ΔH^0, and entropy $-T\Delta S^0$ (kJ mol^{-1}) accompanying the side-chain conformational variations of the C-terminal Asp in achatin-I at the neutral pD at 30°C

	T→G$^+$	T→G$^-$
ΔG^0	4.7 ± 0.1	2.6 ± 0.1
ΔH^0	7.9 ± 0.3	10.1 ± 0.2
$-T\Delta S^0$	−3.2 ± 0.4	−7.5 ± 0.3

ΔG^0, ΔH^0, and $-T\Delta S^0$ for the C-terminal Asp of a natural neuroexcitatory peptide achatin-I (Gly-D-Phe-Ala-Asp) show similar thermodynamic trend to those for the C-terminal Asp in the model Asp peptides. The C-terminal trend of the conformational equilibrium obtained from the model systems is thus confirmed for the Asp in achatin-I with no ionic residues in the sequence neighbor.

SUPPLEMENTARY MATERIAL

An online supplement to this article can be found by visiting BJ Online at http://www.biophysj.org.

We are grateful for the support of this work by the Research Grant-in-Aid from the Ministry of Education, Culture, Sports, Science and Technology (Nos. 13440179 and 13640509).

REFERENCES

Abraham, R. J., and H. J. Bernstein. 1961. The analysis of nuclear magnetic resonance spectra. V. The analysis of deceptively simple spectra. *Can. J. Chem.* 39:216–230.

Abraham, R. J., and K. G. R. Pachler. 1963. The proton magnetic resonance spectra of some substituted ethanes: the influence of substitution on CH-CH coupling constants. *Mol. Phys.* 7:165–182.

Altona, C., R. Francke, R. de Haan, J. H. Ippel, G. J. Daalmans, A. J. A. Westra Hoekzema, and J. van Wijk. 1994. Empirical group electronegativities for vicinal NMR proton-proton couplings along a C–C bond: solvent effects and reparameterization of the Haasnoot equation. *Magn. Reson. Chem.* 32:670–678.

Bartle, K. D., D. W. Jones, and R. L'Amie. 1972. Proton magnetic resonance spectra of amino acids and peptides relevant to wool structure. III. Relative residence times of dipeptides of asparagine, aspartic acid, phenylalanine, and tyrosine. *J. Chem. Soc. Perkin Trans.* 2:650–655.

Booth, H. 1965. The variation of vicinal proton-proton coupling constants with orientation of electronegative substituents. *Tetrahedron Lett.* 6: 411–416.

Burkert, U., and N. L. Allinger. 1982. Molecular Mechanics. American Chemical Society, Washington, DC.

Bystrov, V. F. 1976. Spin-spin coupling and the conformational states of peptide systems. *Prog. Nucl. Magn. Reson. Spectrosc.* 10:41–81.

Cowburn, D., D. H. Live, A. J. Fischman, and W. C. Agosta. 1983. Side chain conformations of oxytocin and vasopressin studied by NMR observation of isotopic isomers. *J. Am. Chem. Soc.* 105:7435–7442.

Dale, B. J., and D. W. Jones. 1975. Unequal populations of amino acid and tripeptide rotamers from 220 MHz PMR spectra. *Spectrochim. Acta A.* 31:83–88.

Dewar, M. J. S., E. G. Zoebisch, E. F. Healy, and J. J. P. Stewart. 1985. AM1: a new general purpose quantum mechanical molecular model. *J. Am. Chem. Soc.* 107:3902–3909.

Feeney, J. 1976. Improved component vicinal coupling constants for calculating side-chain conformations in amino acids. *J. Magn. Reson.* 21:473–478.

Feeney, J., G. C. K. Roberts, J. P. Brown, A. S. V. Burgen, and H. Gregory. 1972. Conformational study of some component peptides of pentagastrin. *J. Chem. Soc. Perkin Trans.* 2:601–604.

Glasoe, P. K., and F. A. Long. 1960. Use of glass electrodes to measure acidities in deuterium oxide. *J. Phys. Chem.* 64:188–190.

Glick, R. E., and A. A. Bothner-By. 1956. Fine splittings in the nuclear magnetic resonance spectra of alkyl derivatives. *J. Chem. Phys.* 25: 362–363.

Gregoire, F., S. H. Wei, E. W. Streed, K. A. Brameld, D. Fort, L. J. Hanely, J. D. Walls, W. A. Goddard, and J. D. Roberts. 1998. Conformational equilibria of β-alanine and related compounds as studied by NMR spectroscopy. *J. Am. Chem. Soc.* 120:7537–7543.

Haasnoot, C. A. G., F. A. A. M. de Leeuw, and C. Altona. 1980. The relationship between proton-proton NMR coupling constants and substituent electronegativities. I. An empirical generalization of the Karplus equation. *Tetrahedron.* 36:2783–2792.

Ishii, H., Y. Fukunishi, Y. Inoue, and R. Chûjô. 1985. β-turn structure and intramolecular interaction of tetrapeptides containing Asp and Lys. *Biopolymers.* 24:2045–2056.

Kainosho, M., and K. Ajisaka. 1975. Conformational analysis of amino acids and peptides using specific isotope substitution. II. Conformation of serine, tyrosine, phenylalanine, aspartic acid, asparagine, and aspartic acid β-methyl ester in various ionization states. *J. Am. Chem. Soc.* 97:5630–5631.

Kamatani, Y., H. Minakata, P. T. M. Kenny, T. Iwashita, K. Watanabe, K. Funase, X. P. Sun, A. Yongsiri, K. H. Kim, P. Novales-Li, E. T. Novales, C. G. Kanapi, H. Takeuchi, and K. Nomoto. 1989. Achatin-I, an endogenous neuroexcitatory tetrapeptide from *Achatina fulica* Férussac containing a D-amino acid residue. *Biochem. Biophys. Res. Comm.* 160:1015–1020.

Karplus, M. 1959. Contact electron-spin coupling of nuclear magnetic moments. *J. Chem. Phys.* 30:11–15.

Karplus, M. 1963. Vicinal proton coupling in nuclear magnetic resonance. *J. Am. Chem. Soc.* 85:2870–2871.

Kent IV, D. R., K. A. Petterson, F. Gregoire, E. Snyder-Frey, L. J. Hanely, R. P. Muller, W. A. Goddard III, and J. D. Roberts. 2002. An NMR and quantum-mechanical investigation of tetrahydrofuran solvent effects on the conformational equilibria of 1,4-butanedioic acid and its salts. *J. Am. Chem. Soc.* 124:4481–4486.

Kim, K. H., H. Takeuchi, Y. Kamatani, H. Minakata, and K. Nomoto. 1991. Structure-activity relationship studies on the endogenous neuroactive tetrapeptide achatin-I on giant neurons of *Achatina fulica* Férussac. *Life Sci.* 48:91–96.

Kimura, T., N. Matubayasi, H. Sato, F. Hirata, and M. Nakahara. 2002. Enthalpy and entropy decomposition of free-energy changes for side-chain conformations of aspartic acid and asparagine in acidic, neutral, and basic aqueous solutions. *J. Phys. Chem. B.* 106:12336–12343.

Kobayashi, J., U. Nagai, T. Higashijima, and T. Miyazawa. 1979. Nuclear magnetic resonance study of side-chain conformation of phenylalanine residue in [Met^5]-enkephalin: solvent, pH, and temperature dependence. *Biochim. Biophys. Acta.* 577:195–206.

Kobayashi, J., T. Higashijima, U. Nagai, and T. Miyazawa. 1980. Nuclear magnetic resonance study of side-chain conformation of tyrosyl residue in [Met^5]-enkephalin: solvent and temperature dependence. *Biochim. Biophys. Acta.* 621:190–203.

Kobayashi, J., T. Higashijima, S. Sekido, and T. Miyazawa. 1981. Nuclear magnetic resonance study on solvent dependence of side chain conformations of tyrosine and tryptophan derivatives. *Int. J. Pept. Protein Res.* 17:486–494.

Kobayashi, J., T. Higashijima, and T. Miyazawa. 1984. Nuclear magnetic resonance analyses of side chain conformations of histidine and aromatic derivatives: solvent and pH dependence. *Int. J. Pept. Protein Res.* 24: 40–47.

Kopple, K. D., and D. H. Marr. 1967. Conformations of cyclic peptides: the folding of cyclic dipeptides containing an aromatic side chain. *J. Am. Chem. Soc.* 89:6193–6200.

Kopple, K. D., and M. Ohnishi. 1969. Conformations of cyclic peptides. II. Side-chain conformation and ring shape in cyclic dipeptides. *J. Am. Chem. Soc.* 91:962–970.

Lit, E. S., F. K. Mallon, H. Y. Tsai, and J. D. Roberts. 1993. Conformational-changes of butanedioic acid as a function of pH as determined from changes in vicinal proton-proton NMR couplings. *J. Am. Chem. Soc.* 115:9563–9567.

Nakamura, A., and O. Jardetzky. 1968. Systematic analysis of chemical shifts in the nuclear magnetic resonance spectra of peptide chains. II. Oligoglycines. *Biochemistry*. 7:1226–1230.

Nielsen, P. A., P.-O. Norrby, T. Liljefors, N. Rega, and V. Barone. 2000. Quantum mechanical conformational analysis of β-alanine zwitterion in aqueous solution. *J. Am. Chem. Soc.* 122:3151–3155.

Nunes, M. T., V. M. S. Gil, and J. Ascenso. 1981. The conformation of succinic acid in aqueous solution studied by ^{1}H and ^{13}C NMR. *Tetrahedron*. 37:611–614.

Pachler, K. G. R. 1967. Die pH-abhängigkeit der kernresonanzspektren der äpfelsäure, o-methyl-äpfelsäure und asparaginsäure. *Z. Anal. Chem.* 39:211–226.

Pachler, K. G. R. 1964. Nuclear magnetic resonance study of some α-amino acids. II. Rotational isomerism. *Spectrochim. Acta*. 20:581–587.

Pople, J. A., W. G. Schneider, and H. J. Bernstein. 1959. High-Resolution Nuclear Magnetic Resonance. McGraw-Hill, New York.

Ramachandran, G. N., C. M. Venkatachalam, and S. Krimm. 1966. Stereochemical criteria for polypeptide and protein chain conformations. III. Helical and hydrogen-bonded polypeptide chains. *Biophys. J.* 6: 849–872.

Schnur, D. M., M. V. Grieshaber, and J. P. Bowen. 1991. Development of an internal searching algorithm for parameterization of the MM2/MM3 force-fields. *J. Comput. Chem.*12:844–849.

Sheinblatt, M. 1966. Determination of amino acid sequence in di- and tripeptides by nuclear magnetic resonance techniques. *J. Am. Chem. Soc.* 88:2845–2848.

Sheppard, N., and J. J. Turner. 1959. High-resolution nuclear-magnetic-resonance spectra of hydrocarbon groupings. II. Internal rotation in substituted ethanes and cyclic ethers. *Proc. R. Soc. Lond. A.* 252: 506–519.

Taddei, F., and L. Pratt. 1964. Proton resonance spectra of some amino acids in aqueous solution. *J. Am. Chem. Soc.* 86:1553–1559.

Williams, D. H., and N. S. Bhacca. 1964. Dependency of vicinal coupling constants on the configuration of electronegative substituents. *J. Am. Chem. Soc.* 86:2472–2473.